Intercomparison of global river discharge simulations focusing on dam operation --- Part II: Multiple models analysis in two case-study river basins, Missouri-Mississippi and Green-Colorado

Manuscript version: Accepted Manuscript
Masaki et al

To cite this article before publication: Masaki et al, 2017, Environ. Res. Lett., at press:
http://dx.doi.org/10.1088/1748-9326/aa57a8

Intercomparison of global river discharge simulations focusing on dam operation — Part II: Multiple models analysis in two case-study river basins, Missouri-Mississippi and Green-Colorado

Yoshimitsu Masaki[1,2], Naota Hanasaki[1], Hester Biemans[3], Hannes Müller Schmied[4,5], Qiuhong Tang[6], Yoshihide Wada[7,8,9,10], Simon N. Gosling[11], Kiyoshi Takahashi[1], and Yasuaki Hijioka[1]

[1] National Institute for Environmental Studies, 16-2 Onogawa, Tsukuba, Ibaraki, 305-8506, Japan

[2] *Current Affiliation*: Graduate School of Science and Technology, Hirosaki University, Bunkyocho-3, Hirosaki, Aomori, 036-8561, Japan

[3] Wageningen University and Research, P.O. Box 47, 6700 AA Wageningen, the Netherlands

[4] Institute of Physical Geography, Goethe-University, Frankfurt, Germany

[5] Senckenberg Biodiversity and Climate Research Centre (BiK-F), Frankfurt, Germany

[6] Key Laboratory of Water Cycle and Related Land Surface Processes, Institute of Geographic Sciences and Natural Resources Research, Chinese Academy of Sciences Beijing 100101, China

[7] NASA Goddard Institute for Space Studies, New York, USA

[8] Center for Climate Systems Research, Columbia University, New York, USA

[9] Department of Physical Geography, Utrecht University, Utrecht, The Netherlands

[10] International Institute for Applied Systems Analysis, Laxenburg, Austria

[11] School of Geography, University of Nottingham, Nottingham NG7 2RD, UK

E-mail: ymasaki@hirosaki-u.ac.jp

Abstract.

We performed a twofold intercomparison of river discharge regulated by dams under multiple meteorological forcings among multiple global hydrological models for a historical period by simulation. Paper II provides an intercomparison of river discharge simulated by five hydrological models under four meteorological forcings. This is the first global multimodel intercomparison study on dam-regulated river flow. Although the simulations were conducted globally, the Missouri-Mississippi and Green-Colorado Rivers were chosen as case-study sites in this study. The hydrological models incorporate generic schemes of dam operation, not specific to a certain dam. We examined river discharge on a longitudinal section of river channels to investigate the effects of dams on simulated discharge, especially at the seasonal time scale. We found that the magnitude of dam regulation differed considerably among the hydrological models. The difference was attributable not only to dam operation schemes but also to the magnitude of simulated river discharge flowing into dams. That is, although a similar algorithm of dam operation schemes was incorporated in

different hydrological models, the magnitude of dam regulation substantially differed among the models. Intermodel discrepancies tended to decrease toward the lower reaches of these river basins, which means model dependence is less significant toward lower reaches. These case-study results imply that, intermodel comparisons of river discharge should be made at different locations along the river's course to critically examine the performance of hydrological models because the performance can vary with the locations.

PACS numbers: 92.40qf, 92.40qh, 92.40qp, 92.40Xx, 92.70Mn

Keywords: river discharge, reservoir, flow regimes, flood control

Submitted to: *Environ. Res. Lett.*

1. Introduction

Humans have constructed approximately 60,000 dams and reservoirs worldwide (Avakyan and Iakovleva, 1998; ICOLD, 2016) with the aim of providing stable access to water resources and preventing riverine disasters. Humans also use riverine water for irrigation, and municipal and industrial purposes. Currently, most world's large rivers are regulated by dams (Nilsson *et al* , 2005). To simulate river discharge affected by human impacts worldwide, global hydrological models (GHMs) implementing dam regulation and water abstraction schemes are necessary (Biemans *et al* , 2011; Bierkens, 2015; Nazemi and Wheater, 2015a, 2015b).

Hydrological simulations are subject to uncertainties arising from various factors. Among them, uncertainties from meteorological forcings and hydrological models are predominant. Firstly, the various global meteorological data sets compiled from observed data with various compilation methodologies may contain different atmospheric conditions (including precipitation), which affects simulated runoff and river discharge (e.g., Müller Schmied *et al* , 2016a). This topic was addressed in Paper I (Masaki *et al* , 2016), which focused on how reservoirs behave during extreme flood events.

Secondly, hydrological models themselves are also sources of uncertainty. Each model implements different schemes for land surface processes (e.g., runoff, evapotranspiration, and infiltration) or river routing processes and also uses different parameters. As a result, even simulations of natural flow (unregulated flow without water withdrawal) differ considerably among GHMs (Haddeland *et al* , 2011). Moreover, human interventions in river flow, such as dam operation and water withdrawal from surface water bodies (e.g., rivers and lakes) and groundwater, are additional sources of uncertainty among GHMs. Although a variety of dam operation strategies exist to meet local water resource requirements/uses, weather conditions, social/political demands and so forth, operational rules and historical records of operations are not available to the public except for a limited number of cases. Therefore, present GHMs incorporate generic schemes of dam operation (e.g., Hanasaki *et al* , 2006; Haddeland *et al* , 2006). Hereafter, the term 'generic schemes' indicates schemes that are not specific to a certain dam but are applicable to a group of dams. Such schemes fundamentally shift the timing of outflows by temporarily storing water without changing the total volume of river flow, insofar as evaporation from open water surfaces of dam reservoirs is considered to be secondary. Generic schemes can successfully reduce errors of simulated river discharge compared with observed discharge. However, practical application of these schemes to actual riverine management has room for further improvement due to their simplification of dam functions (Hanasaki *et al* , 2006).

With the rising use of GHMs, it has become increasingly important to examine their performance through intercomparison (Haddeland *et al* , 2011; Schewe *et al* , 2014; Gosling *et al* , 2016), as well as in terms of water withdrawal (Wada *et al* , 2013) and extreme hydrological events (Dankers *et al* , 2014; Prudhomme *et al* , 2014). However,

no intercomparison of flow regulation has been performed. Moreover, since river flow can be regulated by multiple dams in a river channel, the differences in flow regulation among GHMs should be systematically investigated. In this study, the impacts of dam operation on river flow are examined from upstream to downstream. In addition, it is important to compare simulated and observed discharges to check the model performance in hydrological simulations. For global-scale simulations, comparisons have often been performed at one or a few representative gauge stations for each basin (Nijssen *et al* , 2001; Sperna Weiland *et al* , 2010; Hattermann *et al* , 2016). The station which has a long history of observation near the furthest main-stem reach is favorably used because river flow at these locations is considered to reflect the overall characteristics of the basin. However, since highly regulated rivers have variable seasonal behavior, even among river sectors separated by dams, comparisons and validations of river flow at the furthest reach is insufficient to identify sources of intermodel differences. It is important to perform intercomparisons of regulated river flow by decomposing river channels into sectors from the upper to lower reaches, similar to the longitudinal section analysis of Vörösmarty *et al* (1997).

In this paper (Paper II), we simulated of river discharge under multiple meteorological forcings for the historical period of 1971–2000 using multiple models and examined the characteristics of river discharge regulated by dams. The objectives of this paper are twofold. (1) We examine the effects of different models by comparing the simulated seasonality of river discharge obtained using five GHMs (Section 3.1). Here, we compare the alteration of river flow by dams at the seasonal timescale obtained with multiple models. (2) We also discuss discrepancies among the models under multiple forcings (Section 3.2). To elucidate the effects of dam regulation, we examine the Missouri-Mississippi and Green-Colorado River simulations as case studies. This research was performed under the framework of Phase 2a of the Inter-Sectoral Impact Model Intercomparison Project (ISIMIP).

The structure of this paper is as follows. We outline the data sets and analytical methods in Section 2. The results are presented in Section 3. We discuss the performance and potential problems of the regulated river flow simulations in Section 4. In Section 5, the conclusions are presented.

2. Data and Methods

2.1. Historical meteorological data

Four historical meteorological data sets were used in this study, namely GSWP3 (Kim *et al* , 2014), Princeton PGMFD ver2 (Sheffield *et al* , 2006), WFDEI.gpcc (Weedon *et al* , 2014) and WATCH (Weedon *et al* , 2010), hereafter referred to as GSWP3, PGFv2, WFDEI and WATCH, respectively (Table 1). Since WFDEI.gpcc covers 1979 onward, WFDEI is a combination of WATCH (before 1979) and WFDEI.gpcc (after 1979) in ISIMIP2a. Meteorological variables used in this simulation depend on GHMs

Table 1. Historical meteorological data sets used in this study. The last column shows whether wind-induced precipitation undercatch is corrected. These data sets were re-gridded and distributed by the ISIMIP. [1]Compo *et al* (2011), [2]Kalnay *et al* (1996), [3]Dee *et al* (2011), [4]Uppala *et al* (2005)

Data sets (Abbreviation)	Reanalysis	Precipitation correction	Undercatch
GSWP3	20th Century[1]	GPCC ver6, CRU TS3.21	Corrected
Princeton PGMFD ver.2 (PGFv2)	NCEP-NCAR[2]	CRU TS3.21	Uncorrected
WFDEI.gpcc (WFDEI)	ERA-Interim[3]	GPCC ver5/6	Corrected
WATCH	ERA-40[4]	GPCC ver4	Corrected

(see Table A1), employing different land process schemes. Müller Schmied *et al* (2016a) examined these meteorological data sets and pointed out that differences in chronological decadal trends of meteorological variables caused differences in simulated discharge and evapotranspiration.

2.2. Hydrological simulations

We used the following five GHMs: DBH (Tang *et al* , 2007), H08 (Hanasaki *et al* , 2008a, 2008b), LPJmL (Rost *et al* , 2008; Biemans *et al* , 2011), PCR-GLOBWB (Wada *et al* , 2014) and WaterGAP (Müller Schmied *et al* , 2014, 2016a). All GHMs included dam operation (in consideration of construction year) in their simulation. Their results were available on January, 2016, in the ISIMIP2a framework. In the main, the model settings followed ISIMIP2a protocol (ISIMIP, 2015), although there were some exceptions. All the models covered the globe at a resolution of $0.5^\circ \times 0.5^\circ$ for the period 1971–2000, which is common simulation periods determined by the ISIMIP protocol for the four meteorological data sets. The hydrological state variables of each model at the beginning of 1971 were stabilized (spun-up) using pre-1970 data. River routing was achieved using DDM30 (Döll and Lehner, 2002) (see Section 2.4 later). Analysis settings and model specifications are briefly summarized in Table 2 and Supplement A.1.

To examine anthropogenic effects on river flow, we used simulations called 'varsoc' runs, defined by ISIMIP2a, which included time-varying human interventions (standard analysis settings were dams, water withdrawal, and changes in land use over basins; see also Tables 2 and A1 for details). Historical land use (e.g., type of crop cultivation) is represented annually by Dynamic MIRCA-HYDE. This is a historical extension of MIRCA2000 (Portmann *et al* , 2010), which provides land use data circa 2000 with the extension of time-varying trends given by HYDE3.1 (Goldewijk *et al* , 2011). Dam specifications (location, storage capacity, and construction year) were provided by GRanD ver. 1.1 (Lehner *et al* , 2011a, 2011b). Essentially, the GHMs implemented the dam location data provided as standard data by ISIMIP, which was georeferenced to DDM30. We also used 'nosoc' runs in naturalized, control simulations, in which neither human withdrawals nor dam operation were considered.

Table 2. Hydrological models used in this study. Abbreviations for water use: (Ir) irrigation, (D) domestic, (In) industry, (Mn) manufacturing, (Lv) livestock, and (C) cooling of thermal power plants. See also Table A1 for other specifications of each model. [1]For WaterGAP, Mn + C = In, [2]Calibration covers 54% of global land surface, according to Müller Schmied *et al* (2016a), [3]See also the Supplement A2.

GHM	Water use	Calibration	River routing	Dam operation scheme	Evaporation from water surface of dams
DBH	Ir	No	linear reservoir, DDM30	Hanasaki *et al* (2006)[2]	No
H08	Ir,D,In	No	linear reservoir, DDM30	Hanasaki *et al* (2006)[2] (active only for flood prevention scheme)	No
LPJmL	Ir,D,In,Lv	No	linear reservoir, DDM30	Biemans *et al* (2011)	Considered
PCR-GLOBWB	Ir,D,In,Lv	No	travel-time routing	Wada *et al* (2014)	Considered
WaterGAP	Ir,D,Mn,Lv,C[1]	Calibrated on long-term mean annual discharge[2]	linear reservoir, DDM30	Hanasaki *et al* (2006)[3]	Considered

Some GHMs used analysis settings that were different from the standard ones. As shown in Table 2, four of the five models included human withdrawals other than irrigation. WaterGAP adopts static land use but varies irrigation areas yearly. Regarding the dam location data, some GHMs relocated dams in consideration of different priorities (Table A2; see also comparison maps by Müller Schmied *et al* (2016b)).

2.3. Post-simulation analysis

In this paper, we focused mainly on the climatological seasonality of river discharge for two major global rivers, and compared simulated data with observations. We aggregated both simulated and observed daily river discharge over three-month periods: December to February (DJF), March to May (MAM), June to August (JJA), and September to November (SON), which correspond to winter, spring, summer, and fall, respectively.

The observed discharge data were obtained from the archive of the Global Runoff Data Centre (GRDC) and the United States Geological Survey (USGS). To compare simulated and observed discharge, we georeferenced the river gauge station to DDM30 so that the catchment area of the station agreed with that of DDM30. We divided the analysis period 1971–2000 into three 10-yr time spans in our analysis because not all gauge stations had been in operation over the entire 30-yr analysis period. To utilize as

many gauge stations as possible for comparison with simulated discharge and to suppress meteorological year-to-year variability, we considered the 10-year period is adequate for our purpose.

2.4. Case studies

In this paper, the Missouri-Mississippi and Colorado River basins were chosen as case studies. We chose these river basins because (1) historical river discharge records are available, particularly for gauge stations in different river sectors separated by large dams, (2) there is clear seasonality in the river discharge, (3) the flow is significantly regulated by large reservoirs, and (4) both river basins have large catchment areas so that differences in geographical characteristics inside these river basins can be resolved at a resolution of $0.5° \times 0.5°$. In fact, the levels of flow regulation are 15.5% and 280% for the Mississippi and Colorado River Basins, respectively, estimated as the percentage of total reservoir capacity within a river system relative to volumetric annual discharge, following Nilsson *et al* (2005)(Table S1). Moreover, historical reservoir operation records for major dams on these rivers are available. In this study, we performed both multiforcing and multimodel comparisons for the Missouri-Mississippi River and a multimodel comparison for the regulated flow of the Green-Colorado River.

To analyze discharge on a longitudinal section of these rivers, we allocated the sequential cell number (SCN) along the main channel from the upper to the lower reaches (Figure 1) of these rivers. Figure 1 also shows the land cells with simulated annual mean river discharge (varsoc run) > 100 m^3/s for each GHM. Since these major rivers have high water flux, land cells with low discharge (those in dark gray in Figure 1) were not considered as part of the main stem in each GHM.

2.4.1. Missouri-Mississippi River Basin The Mississippi River is the third largest river basin in the world (including its tributaries) and travels through a wide range of climates and geography from snow-packed mountainous areas to temperate plains. The flow has clear natural seasonality due to spring snowmelt in the mountainous areas and heavy rain in the plains during warm months, but is heavily regulated by large dams on the Missouri River.

Large dams have been constructed since the mid-20th century to maintain the riverine environment. Five large dams (Table A3) have significant impacts on seasonal river flow due to their large storage capacity (see US Army Corps (2006) for dam management details). In this study, historical dam operation data obtained from the US Army Corps of Engineers (Northwest Division) were also used in the analysis. To compare simulated and observed discharges, 12 gauge stations (Table A4 and Fig. A1) along the Missouri-Mississippi River were used.

2.4.2. Green-Colorado River Basin The Colorado River starts in the Rocky Mountains, travels through a dry region, and flows into the Gulf of California. The river is known

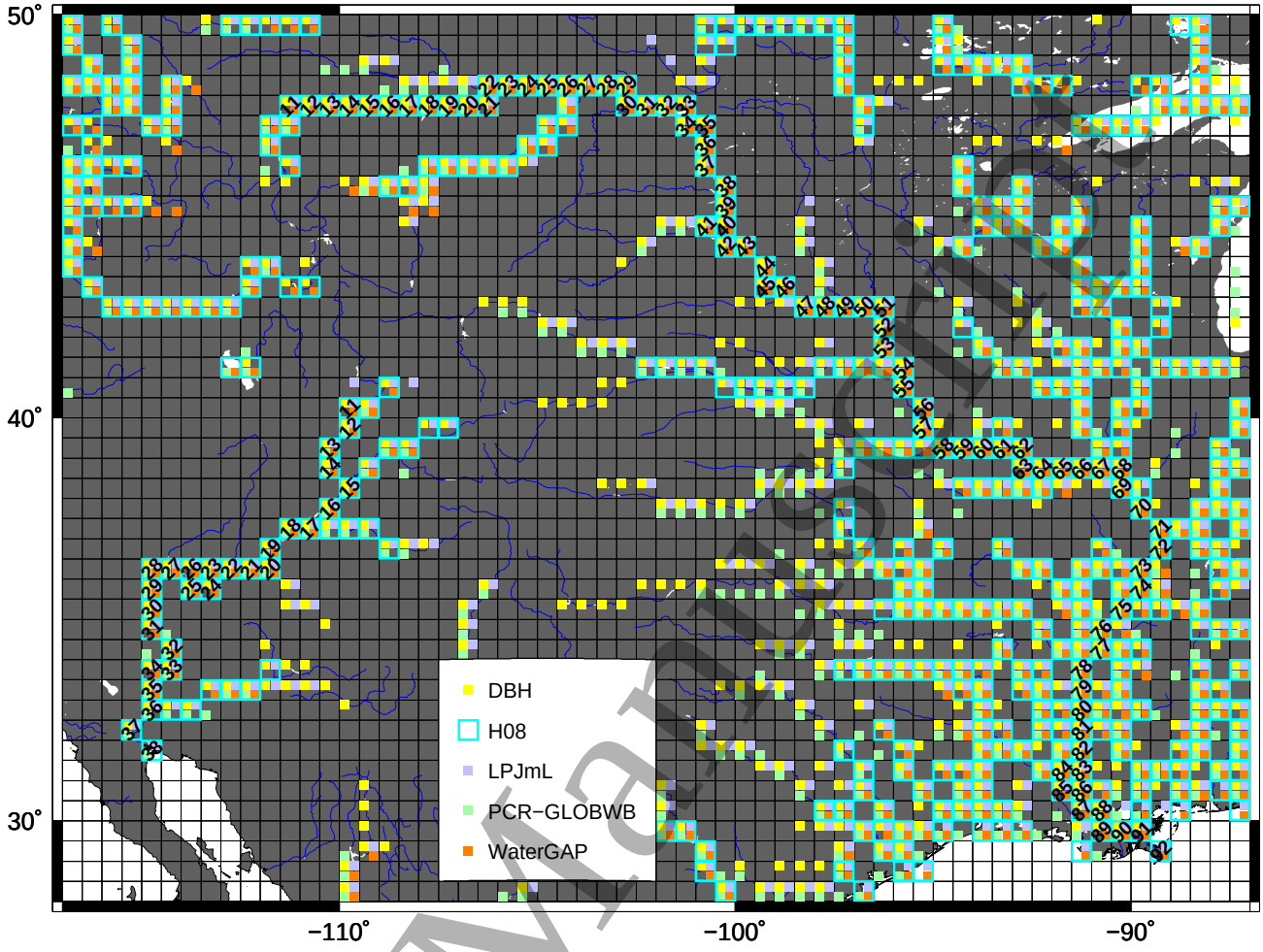

Figure 1. Example of major river channels implemented in each global hydrological model (GHM) in the central part of the United States. Black grid lines separate land cells with the dimensions of $0.5° \times 0.5°$. To visualize the channels, symbols were added to the land cells with an annual average discharge (varsoc run) of greater than 100 m^3/s. Different symbols were marked for each GHM (see the inserted box). The numbers superimposed on the land cells show the sequence of land cells along the longest stems of the Missouri-Mississippi (flowing from the top center to the bottom right in the map) and Green-Colorado (from the center to bottom left) Rivers. Owing to the instability of hydrological simulation over a small catchment area, we omitted the first 10 cells of the river from the source in the intermodel comparison.

to be one of the most regulated rivers in the world (Glen Canyon and Hoover Dams; see Table A5). We chose this basin expecting that uncertainty in operation schemes would be clearly detected in simulated river discharge because of the high ratio of the dam capacity to the annual discharge. Moreover, the water is also supplied for irrigation and municipal use in the basin and its neighborhood. Thus, hydrological simulation using a generic dam operation scheme in this river basin is not only challenging, but also useful to examine intermodel discrepancies due to dam operation. Historically, the discharge of

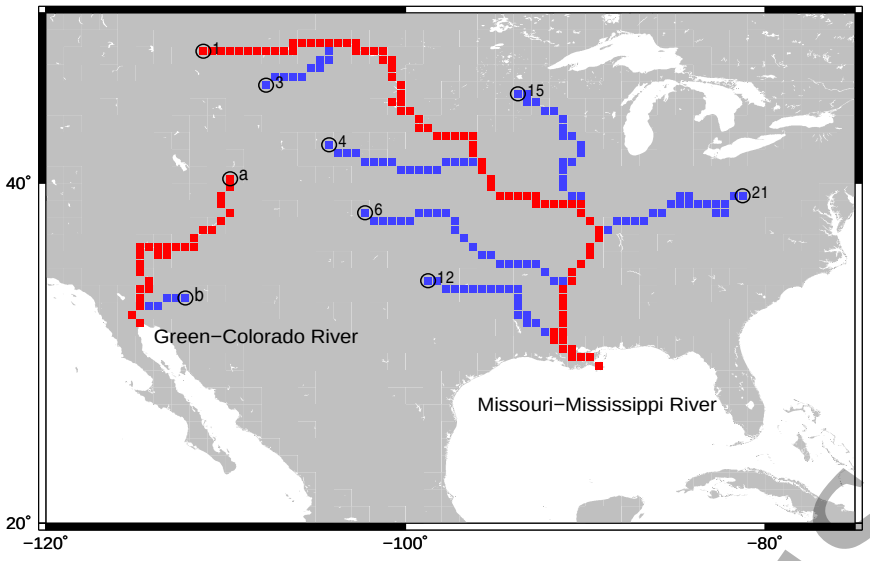

Figure 2. Major tributaries (indicated in blue) directly flowing into the Missouri-Mississippi or Green-Colorado Rivers (red). IDs were assigned to each tributary. The individual river names are: (1) Missouri, (3) Yellowstone, (4) Platte, (6) Arkansas, (12) Red, (15) (Upper) Mississippi, and (21) Ohio for the Missouri-Mississippi River System, and (a) Green and (b) Gila for the Green-Colorado River System. Only river sectors more than 10 cells from the source are indicated.

this river system was drastically changed by the construction of Hoover Dam (storage: 3.670 $\times 10^{10}$ m^3) in 1935 and Glen Canyon Dam (storage: 2.507 $\times 10^{10}$ m^3) in 1963. The peak river flow in the upper basin occurs in spring due to snowmelt. Note that the Green River is also regulated by Flaming Gorge Dam (storage: 4.336 $\times 10^{9}$ m^3).

We focused on a longitudinal section along the Green and Colorado Rivers, the longest reach of the river system. Five gauge stations (Table A6) were used for comparison.

3. Results

3.1. Intercomparison of the seasonal fraction of river discharge among hydrological models

The seasonal fraction of river discharge varied among the GHMs. To visualize the effects of dam operation on the seasonal flow at different river sectors fragmented by dams, we drew a longitudinal section along each river channel (Sections 3.1.1 and 3.1.2) and interpreted the results with hydrographs (Section 3.1.3). In this section, we used the simulation results forced by GSWP3 for simplicity. Since the seasonality of main channel flow is altered not only by dams but also by the confluence of major tributaries under natural conditions, we also accounted for major tributaries in the interpretation (see also Figure 2).

3.1.1. Missouri-Mississippi River Figure 3 shows the results of the seasonal fraction of discharge for the Missouri-Mississippi River. The horizontal axis gives the location along the main stem in terms of the SCN from the upper (leftward) to lower (rightward) reaches. For each GHM, seasonal fractions relative to annual discharge are shown, with corresponding heights presented in different colors. Although only river discharge for the decade 1971–1980 is shown, similar seasonality was observed in other decades. Figure 4 extracts the seasonal fractions at three representative sites on the channel from Figure 3 for intermodel comparison.

Among the GHMs, a high flow was generally observed in spring-summer due to mountain snowmelt in the upper reaches. As the river flows down to the plains, the climate becomes warmer and precipitation increases, peaking in summer. An evenly distributed flow throughout the seasons can be observed in the middle reach of the Mississippi River. Seasonal behavior also changes downstream from the confluence of tributaries, such as the Arkansas (#6), (Upper) Mississippi (#15) and Ohio (#21) Rivers. In the lower reaches of the Mississippi River, water is abstracted for irrigation (Figure C2 includes only the results from H08), but withdrawal is sufficiently smaller than the river discharge so it did not markedly alter the river flow seasonality.

The intermodel comparison of river flow seasonality frequently showed the greatest proportion of river flow in spring to summer, but the seasonal fraction of river flow differed among the GHMs (Figures 3 and 4). H08 had higher flow in spring, whereas DBH had higher flow in summer. Note that high annual variations can be seen in the upper reaches, whereas there were lower annual variations among the GHMs in the lower reaches.

Next, we focused on flow regulation by dams. Judging by the discontinuity in the seasonal fraction of river flow due to the impact of dams (e.g., Fort Peck Dam at SCN 22), the magnitude of seasonal flow regulation differed markedly among the GHMs. H08, LPJmL, and WaterGAP introduced greater seasonal flow modulation than DBH and PCR-GLOBWB. Intermodel differences in seasonality were weakened as the river flowed downstream, possibly because of flows merging according to various seasonal behaviors of tributaries. The seasonality of the five-GHM ensemble mean reproduced the seasonality observed at land cells where gauge stations were located. However, discontinuity at dams was unclear as a result of averaging. Moreover, whether regulated flows began in land cells where dams were located, or in an adjacent cell, depended on the GHM.

Based on the observed seasonality at the gauges, each model has advantages and disadvantages with respect to reproducing seasonality along the whole channel (Table C1). Even if a GHM performs well for some river sectors, it does not perfectly reproduce seasonality for other river sectors. Note that the seasonality of WaterGAP was not affected from calibration because WaterGAP was calibrated with long-term mean annual discharge, not seasonal discharge.

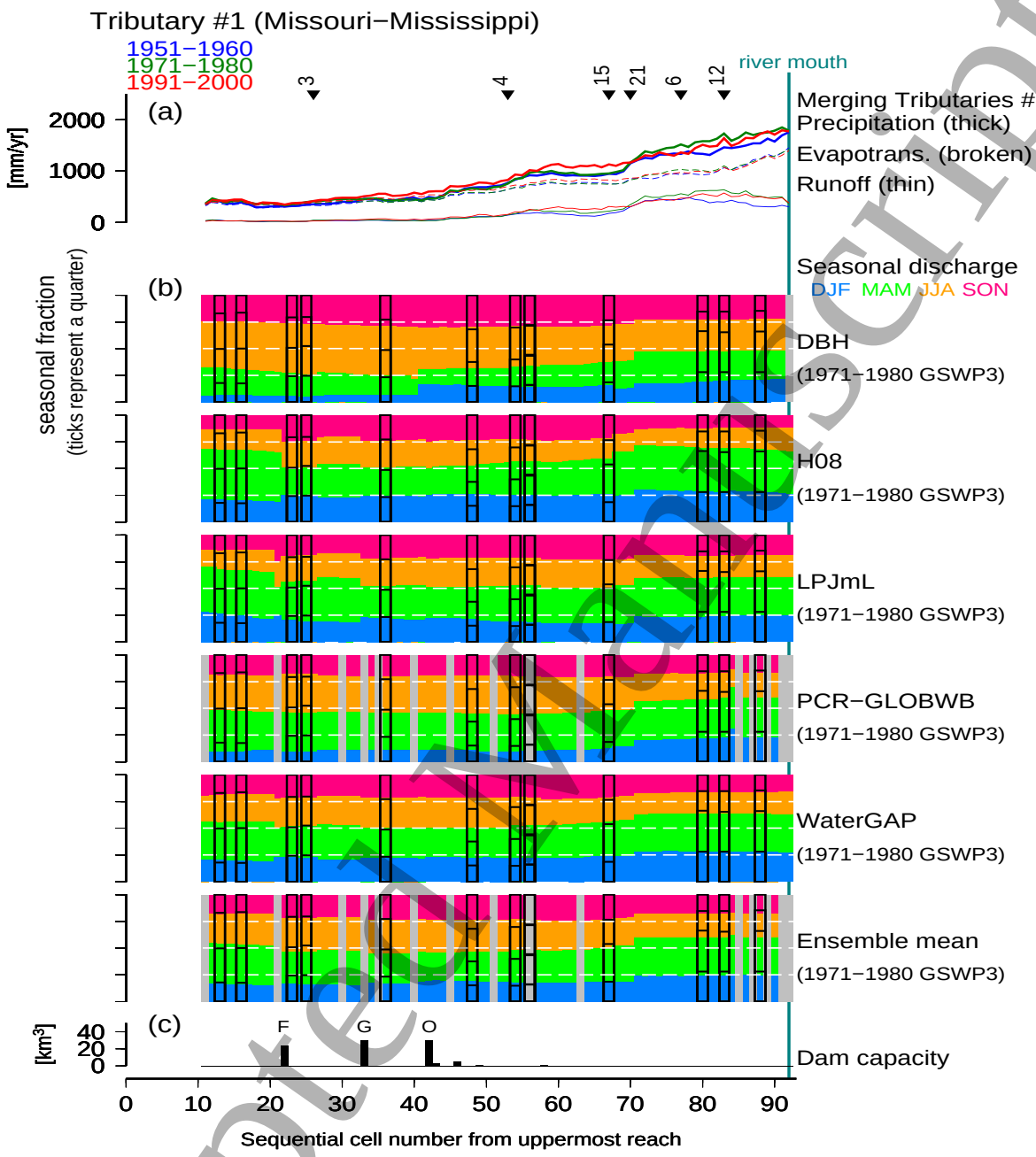

Figure 3. Seasonal fraction of river discharge simulated using five hydrological models (varsoc run) and basic hydroclimatological parameters (runoff and evapotranspiration by H08) on a longitudinal section along the Missouri-Mississippi River. The horizontal axis gives the sequential cell number (SCN) from the uppermost reach of the Missouri River (as indicated in Figure 1). (a) Historical changes in precipitation, evapotranspiration, and runoff are shown as blue, green, and red lines for 1951–1960, 1971–1980, and 1991–2000, respectively. Tributaries that meet the Missouri-Mississippi River are indicated by numbers in the upper panel. See also Tributary IDs in Figure 2. (b) The seasonal fraction of river flow for 1971–1980 is indicated by different colors: cyan (DJF), green (MAM), orange (JJA), and magenta (SON). Gray cells indicate land cells through which the river channels used by each GHM did not pass (see Figure 1). The observed seasonality at gauge stations is indicated by the ladder-shaped boxes. White broken lines show equal partitions among seasons (25% each). (c) Dam capacity is indicated in the same colors as (a). Fort Peck (F), Garrison (G), and Oahe (O) Dams are located at SCNs 22, 33, and 42, respectively.

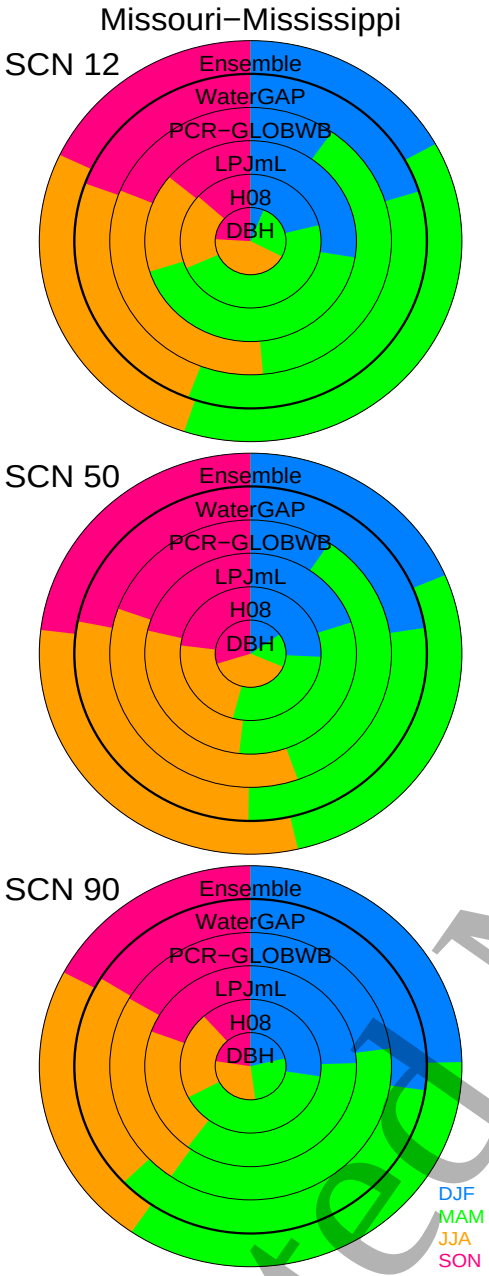

Figure 4. Intermodel comparison of seasonal fraction of river discharge, shown in Figure 3, at three selected sites on the Missouri-Mississippi River. Three sites are representative of the upper (SCN 12), middle (SCN 50) and lower (SCN 90) reaches. The seasonal fractions of river flow for 1971–1980 are indicated by different colors: cyan (DJF), green (MAM), orange (JJA), and magenta (SON). The outermost circle represents the ensemble mean of the five GHMs.

3.1.2. Green-Colorado River Figure 5 shows the results for the Green-Colorado River for 1971–1980. Since the seasonality of the observed river discharge changed somewhat over the decades, we also included the results for 1991–2000 in the Supplement (Figure C1). The seasonal fractions at two representative sites on the channel are shown in Figure 6. As mentioned earlier, reproducing the seasonal flow of the Colorado River is challenging for all hydrological models, owing to multiple human interventions. The simulated discharge of the Green River tended to be higher in spring than in other seasons, whereas the observed discharge was higher in both spring and summer. At Glen Canyon Dam (SCN 17) in the Colorado River, the seasonal flow variation was markedly reduced. All the GHMs showed less seasonality toward the river mouth. In the lower reaches, river water was abstracted for irrigation (which can also be seen in Figure C3 in the results for H08), but the withdrawal was sufficiently small compared with the river discharge. Thus, irrigation was hardly noticeable in the river flow seasonality.

The magnitude of flow regulation at the dams differed among the models. H08, LPJmL, and WaterGAP showed strong flow regulation, whereas the other models showed weaker regulation. The five-GHM ensemble mean reproduced the observed seasonality with reasonable accuracy. We note that discontinuity in the seasonality simulated with WaterGAP at the three cells from the lowermost reach was generated by strong calibration of the simulated discharge (reduced to ca. 25%), intended to match the long-term mean of the observed annual discharge. This feature was also observed as a sudden decrease in annual discharge at SCNs 36–38 in Figure 1.

3.1.3. Different magnitudes of flow regulation across GHMs These results showed that flow regulation differed considerably across the GHMs. What explains these differences? We examined their causes by using simulated hydrographs at sites downstream of large dams (Fort Peck Dam in the Missouri River and Glen Canyon Dam in the Colorado River). We focused on how the river flow was modulated by the dams in each GHM. For this purpose, we analyzed land cells where the dams are located in each GHM because the location could differ by one cell upstream or downstream along the main channel among the GHMs.

Tables 3 and 4 show mean river discharge at the dam sites. The ranges of the forcing-ensemble means among the GHMs were markedly larger than those of the GHM-ensemble means among the meteorological forcings. The ranges of the final columns were 725.3 m^3/s for Fort Peck Dam and 669.9 m^3/s for Glen Canyon Dam, whereas those of the final rows were 105.6 m^3/s and 227.3 m^3/s, respectively. These results indicate that the spread of the simulated river discharge depended more strongly on the GHM than on the meteorological forcing, which is consistent with published intercomparison studies using multiple general circulation models and multiple GHMs (e.g., Wada *et al* , 2014; Hattermann *et al* , 2016). These large intermodel differences in mean discharge were not attributable to the variations in catchment area that resulted from differences in the dam locations used by the GHMs. If we re-evaluate the range of mean river discharge at the common land cell (SCN 22 for Fort Peck Dam and SCN 17 for Glen

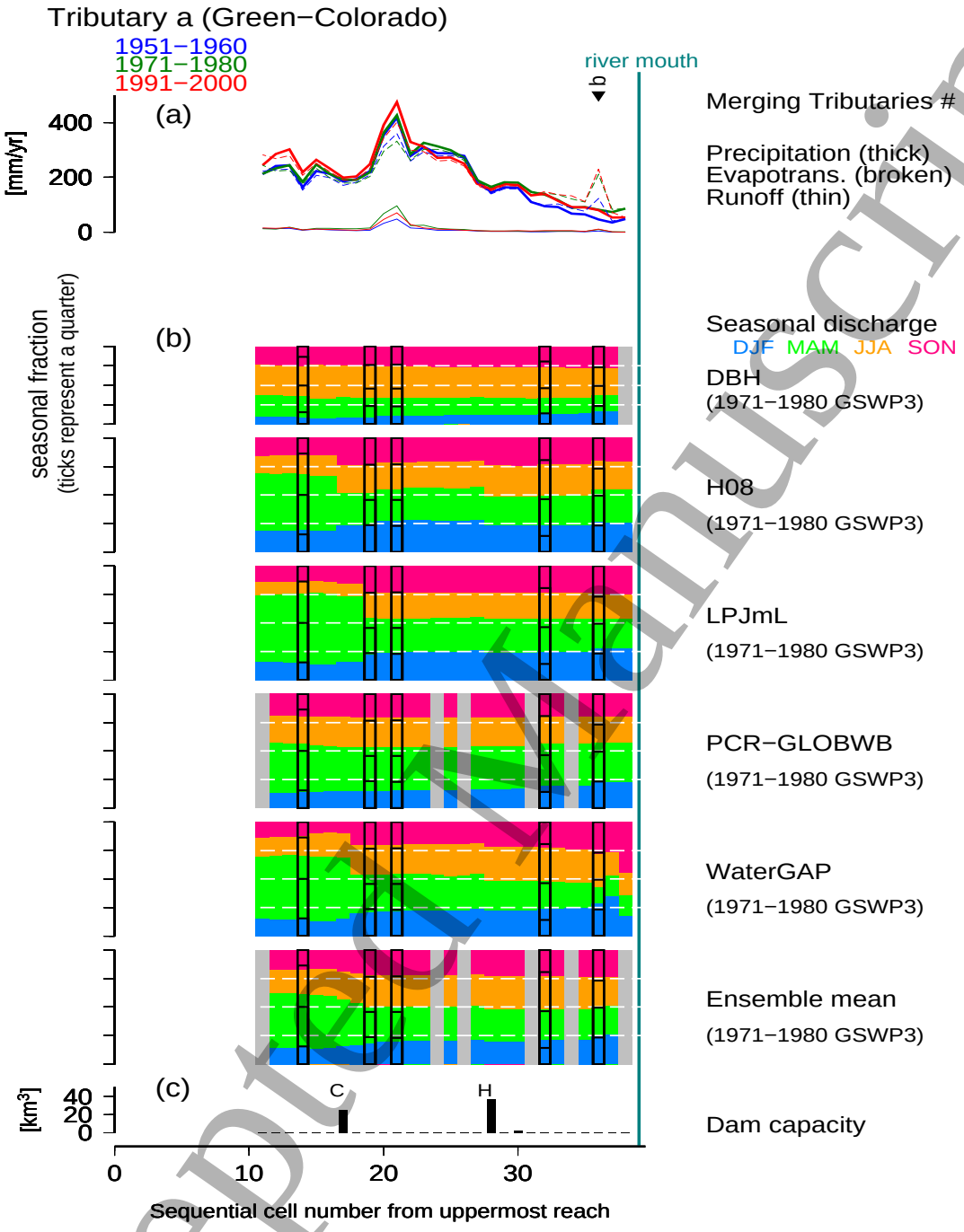

Figure 5. Same as Figure 3 but for the longitudinal section along the Green-Colorado River, with river discharge data for 1971–1980. The horizontal axis gives the SCN from the uppermost reach of the Green River (as indicated in Figure 1). Glen Canyon (C) and Hoover (H) Dams are located at SCNs 17 and 28, respectively.

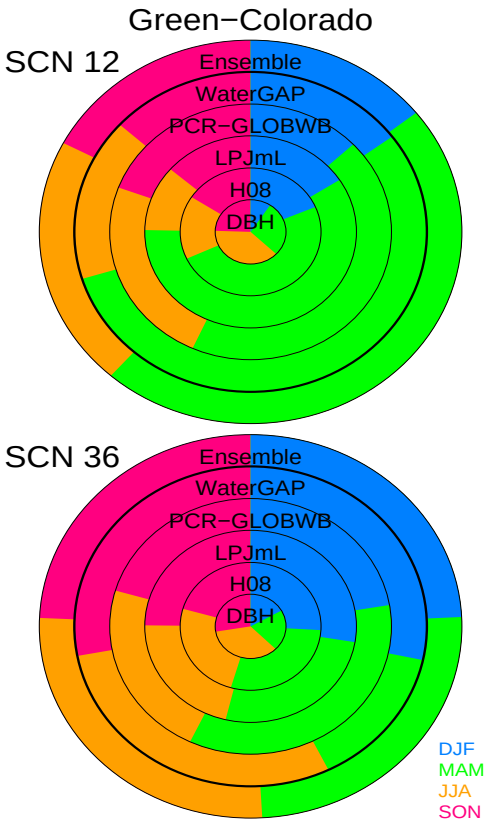

Figure 6. Intermodel comparison of the seasonal fraction of river discharge shown in Figure 5 at two selected sites on the Green-Colorado River. Two sites are representative of the upper (SCN 12) and lower (SCN 36) reaches. A similar representation to Figure 4 is used.

Canyon Dam, following the standard dam data distributed by ISIMIP, the intermodel ranges (725.3 m^3/s for Fort Peck Dam and 642.2 m^3/s for Glen Canyon Dam) are still larger than the interforcing ranges (112.1 m^3/s and 229.0 m^3/s, respectively).

Figure 7 shows hydrographs and cumulative discharge at the dam sites (note that a plot of the cumulative discharge of natural flow with a longer time is known as a mass curve or Rippl diagram, which is useful for designing the dam capacity (Rippl, 1883; Adeloye, 2012)). By comparing regulated flow with natural flow, we found that seasonal variability was suppressed by dam regulation, i.e., decreased discharge in the high-flow season and increased discharge in the low-flow season. As a result, the mass curve in the high-flow season (spring to summer) had a more gradual slope and less curvature for regulated flow than for natural flow.

DBH gave larger estimates of the mean river discharge for 1971–1980 than the other GHMs (Figure 7; Tables 3 and 4). Since the effective magnitude of flow regulation by dams is given approximately by the ratio of dam capacity to mean annual discharge, DBH regulates river flow more weakly than the other models. This is one reason why

Table 3. Mean river discharge at Fort Peck Dam for 1971–1980. The numbers in brackets show the turnover (detention) period required to fill the nominal dam capacity (2.356×10^{10} m^3) at the rate of the mean river discharge.

GHM	SCN	GSWP3		PGFv2		WFDEI		WATCH		Ensemble	
		m^3/s	(d)	m^3/s	(d)	m^3/s	(d)	m^3/s	(d)	m^3/s	(d)
DBH	22	832.4	(327.6)	914.2	(298.3)	1137.7	(239.7)	1157.1	(235.7)	1010.4	(269.9)
H08	22	275.6	(989.4)	218.9	(1245.7)	322.3	(846.1)	323.9	(841.9)	285.1	(956.5)
LPJmL	21	454.3	(600.2)	495.7	(550.1)	614.0	(444.1)	618.3	(441.0)	545.6	(499.8)
PCR-GLOBWB	22	415.2	(656.8)	402.5	(677.5)	401.0	(680.0)	383.4	(711.2)	400.5	(680.9)
WaterGAP	21	287.5	(948.5)	327.1	(833.6)	295.4	(923.1)	310.4	(878.5)	305.1	(893.8)
Ensemble		453.0	(602.0)	471.7	(578.1)	554.1	(492.1)	558.6	(488.2)	509.3	(535.4)

Table 4. Mean river discharge at Glen Canyon Dam for 1971–1980. The numbers in brackets show the turnover (detention) period required to fill the nominal dam capacity (2.507×10^{10} m^3) at the rate of the mean river discharge.

GHM	SCN	GSWP3		PGFv2		WFDEI		WATCH		Ensemble	
		m^3/s	(d)	m^3/s	(d)	m^3/s	(d)	m^3/s	(d)	m^3/s	(d)
DBH	17	849.7	(341.5)	1024.2	(283.3)	1349.4	(215.0)	1386.5	(209.3)	1152.5	(251.8)
H08	17	549.4	(528.1)	600.2	(483.4)	772.0	(375.9)	797.8	(363.7)	679.8	(426.8)
LPJmL	19	882.1	(328.9)	1056.8	(274.6)	1151.2	(252.1)	1150.8	(252.1)	1060.2	(273.7)
PCR-GLOBWB	17	590.9	(491.1)	700.3	(414.3)	667.2	(434.9)	632.9	(458.5)	647.8	(447.9)
WaterGAP	18	447.1	(649.0)	487.9	(594.7)	507.8	(571.4)	487.6	(595.1)	482.6	(601.2)
Ensemble		663.8	(437.1)	773.9	(374.9)	889.5	(326.2)	891.1	(325.6)	804.6	(360.6)

the flow regulation was marginal in DBH. On the other hand, the mean discharge of LPJmL at Glen Canyon Dam was comparable to that of DBH (Table 4). However, the hydrographs (Figure 7) showed that its seasonal peak flow was larger and lasted for a shorter duration than LPJmL. The clear seasonal contrast in the LPJmL simulation helped the dam to act as a stronger regulator than it did in the DBH simulation.

The magnitude of flow regulation at the seasonal scale was not determined principally by the dam manipulation scheme adopted by each GHM. Although DBH, H08, and WaterGAP implemented the flow regulation scheme proposed by Hanasaki *et al* (2006), the simulated flow regulation contrasted clearly between DBH (with weak regulation) and H08 or WaterGAP (with strong regulation). Dam outflow is primarily determined as a function of the mean annual inflow in the scheme of Hanasaki *et al* (2006) (see A.1 in the Supplement). Therefore, simulated variables such as dam water storage at the beginning of the operational year, water demand (dams for irrigation purposes only), inflow variability, and the consequent differences in water storage are considered as the actual causes of the discrepancies in seasonal-scale dam flow regulation among the GHMs.

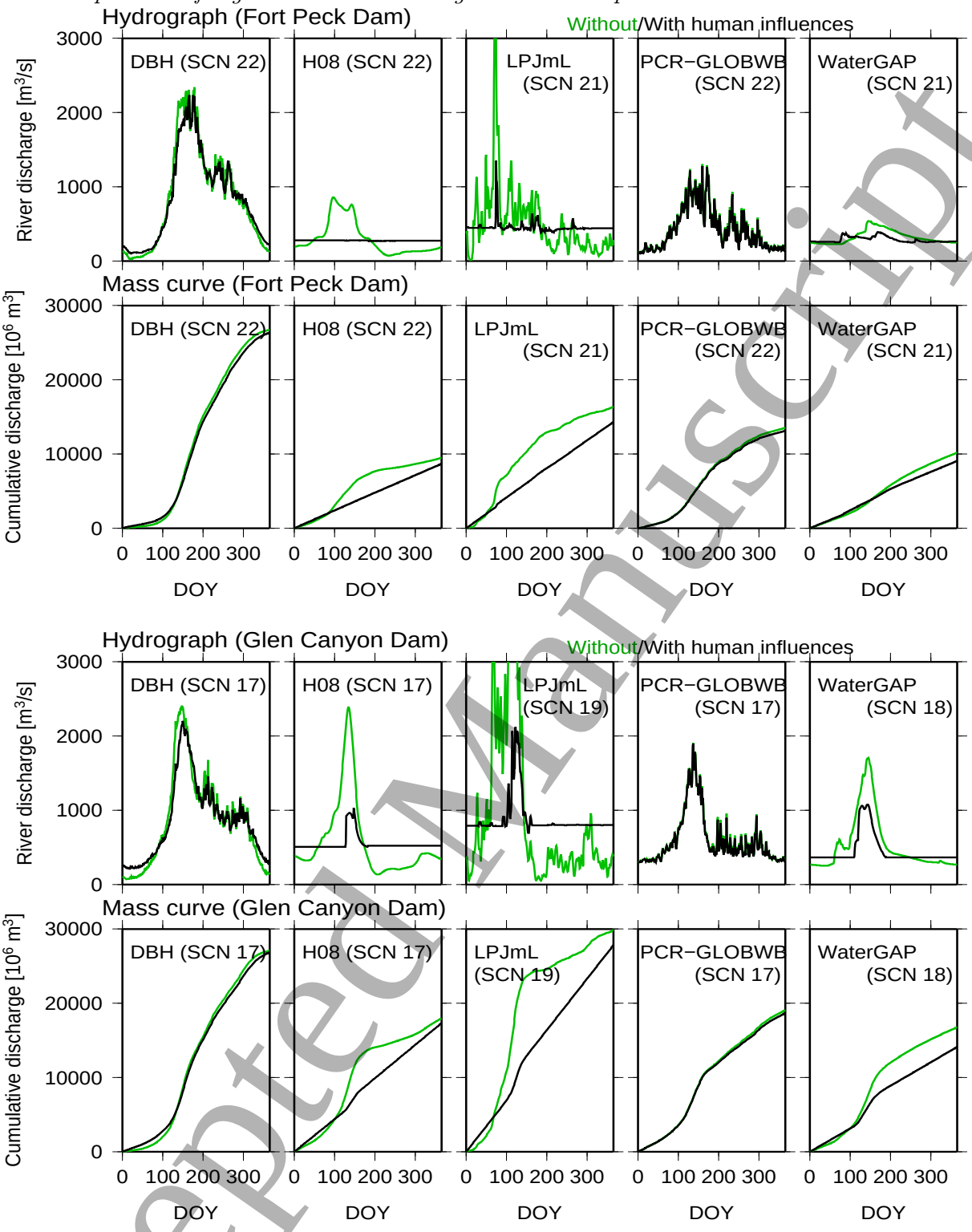

Figure 7. Hydrograph and cumulative discharge (so-called mass curve or Rippl diagram) based on the mean daily discharge for 1971–1980 at a site downstream of Fort Peck and Glen Canyon Dams. Green and black lines show the results of the nosoc (without human influences) and varsoc (with water withdrawal and dam regulation) runs. The horizontal axis is the day of the year (DOY in calendar year). The meteorological forcing is GSWP3. Horizontally aligned panels show the results of each GHM. From left to right, DBH, H08, LPJmL, PCR-GLOBWB, and WaterGAP. The location (shown as SCN) is indicated in each panel.

3.2. Differences in the seasonal fraction of river discharge under four meteorological forcings

The discrepancies in flow regulation among the GHMs also varied with the rivers' courses. To quantify the variance in the seasonal fraction of river discharge among the five GHMs, we calculated the standard deviation (SD) of the five GHMs from their ensemble mean for each season under four meteorological forcings. Figures 8 and 9 show the results for the Missouri-Mississippi and Green-Colorado Rivers, respectively. Since the seasonal fraction is a normalized value by the annual discharge, the fraction is comparable with ones at different locations.

Three major characteristics were observed in the results for the multiple GHMs and forcings. First, the obtained SDs were generally independent of the meteorological forcing for a large proportion of the river sectors. This indicates that SDs were explained primarily by differences among GHMs rather than meteorological forcings. This finding is consistent with Tables 3 and 4 at the two selected sites. Second, larger SDs were observed more frequently in upper reaches than in lower reaches: SDs generally decreased downstream. This means that even if GHMs generally agree in the lower reaches, larger discrepancies may still exist in the upper reaches. Third, SDs in absolute terms tended to be larger during high-flow seasons (spring to summer for both rivers) than during low-flow seasons (fall to winter).

Next, we examined the differences in the results between natural and regulated flows. Overall, natural flow (crosses) tended to have slightly higher SD values than regulated flow (filled circles) for MAM, JJA, and SON. This implies that implementing dam regulation schemes contributes to small discrepancies among the GHM results. Large intermodel discrepancies in natural flow were observed more frequently in high-flow seasons than in low-flow seasons (e.g., Figure 7) because of high variability in precipitation events. Dams contributed to a flattening of the variability and redistribution of water among the seasons, which lowered the SD of regulated flow during high-flow seasons. By contrast, the regulated flow for DJF had slightly higher SD values than the natural flow in some river sectors. Winter had the lowest discharge for both rivers because of the accumulation of snowpack in mountainous areas and the weak rainfall over the catchment area. Thus, a stable and low flow was observed for all the GHMs, along with a similar temporal profile. Dam operation in low-flow seasons increased the discharge, but its amplification was different among the GHMs (Figure 7). This explains the larger SDs for regulated flow compared to natural flow for DJF.

Note that these findings did not always hold true. For example, at Fort Peck Dam (SCN 22) on the Missouri-Mississippi River (Figure 8), the SD of the regulated flow discontinuously increased downstream for DJF but decreased for MAM and SON. Because flow seasonality drastically changed into less seasonal variability by the dam (Figure 3), MAM seasonal fraction of discharge converged among the GHMs, even though MAM was a high-flow season for natural flow.

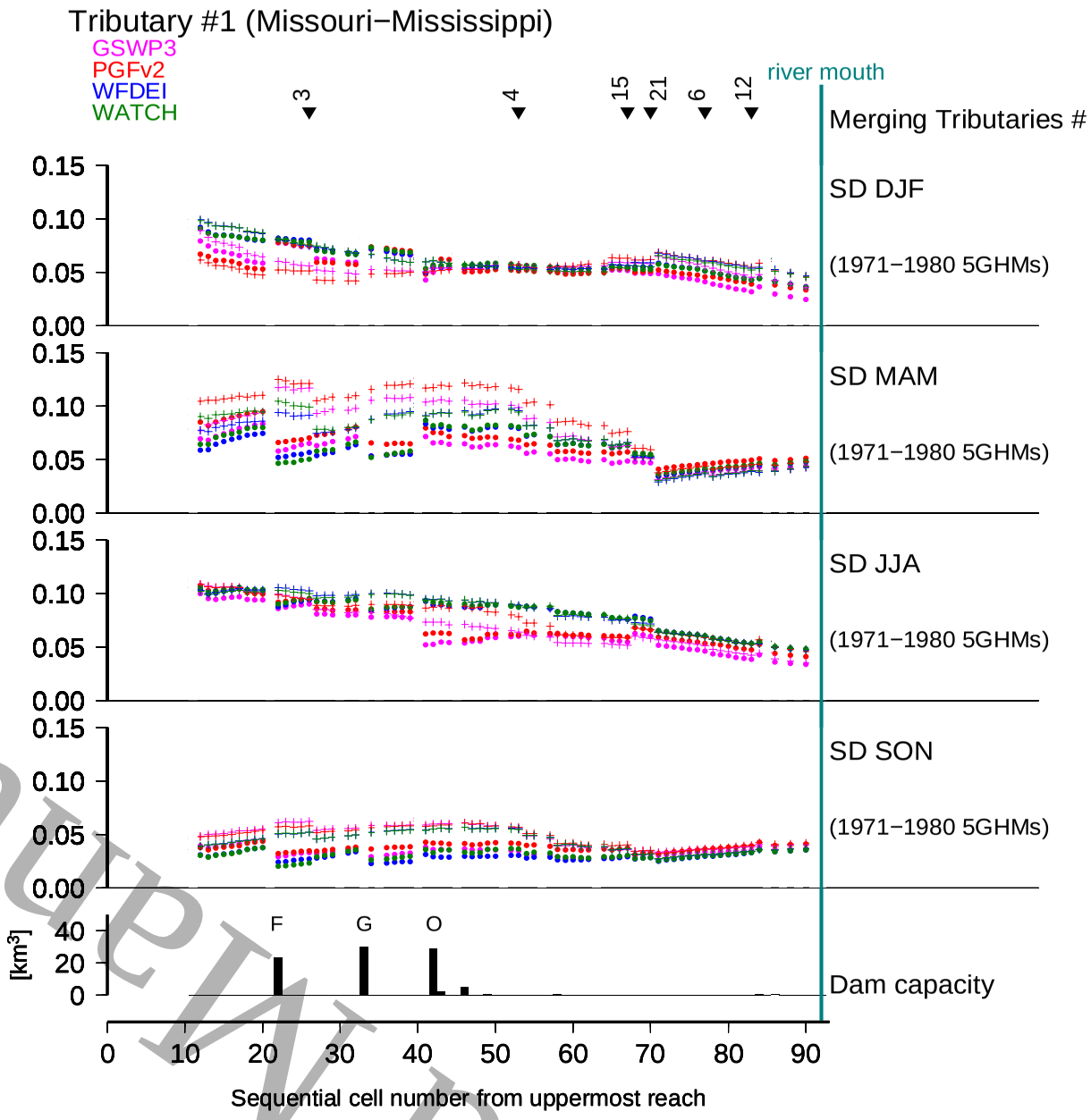

Figure 8. Standard deviations (SDs) of the seasonal fraction of river discharge in the longitudinal section along the Missouri-Mississippi River among the five GHMs. The seasonal fraction for each GHM is shown in Figure 3. The horizontal axis is the SCN from the uppermost reach of the Missouri River (as indicated in Figure 1). Meteorological forcing data sets are indicated by different colors: purple (GSWP3), red (PGFv2), blue (WFDEI), and green (WATCH). Results of the varsoc and nosoc runs are shown by filled circles and crosses, respectively. Blank cells indicate that SDs were not calculated because of missing data for some GHMs. Fort Peck (F), Garrison (G), and Oahe (O) Dams are located at SCNs 22, 33, and 42, respectively.

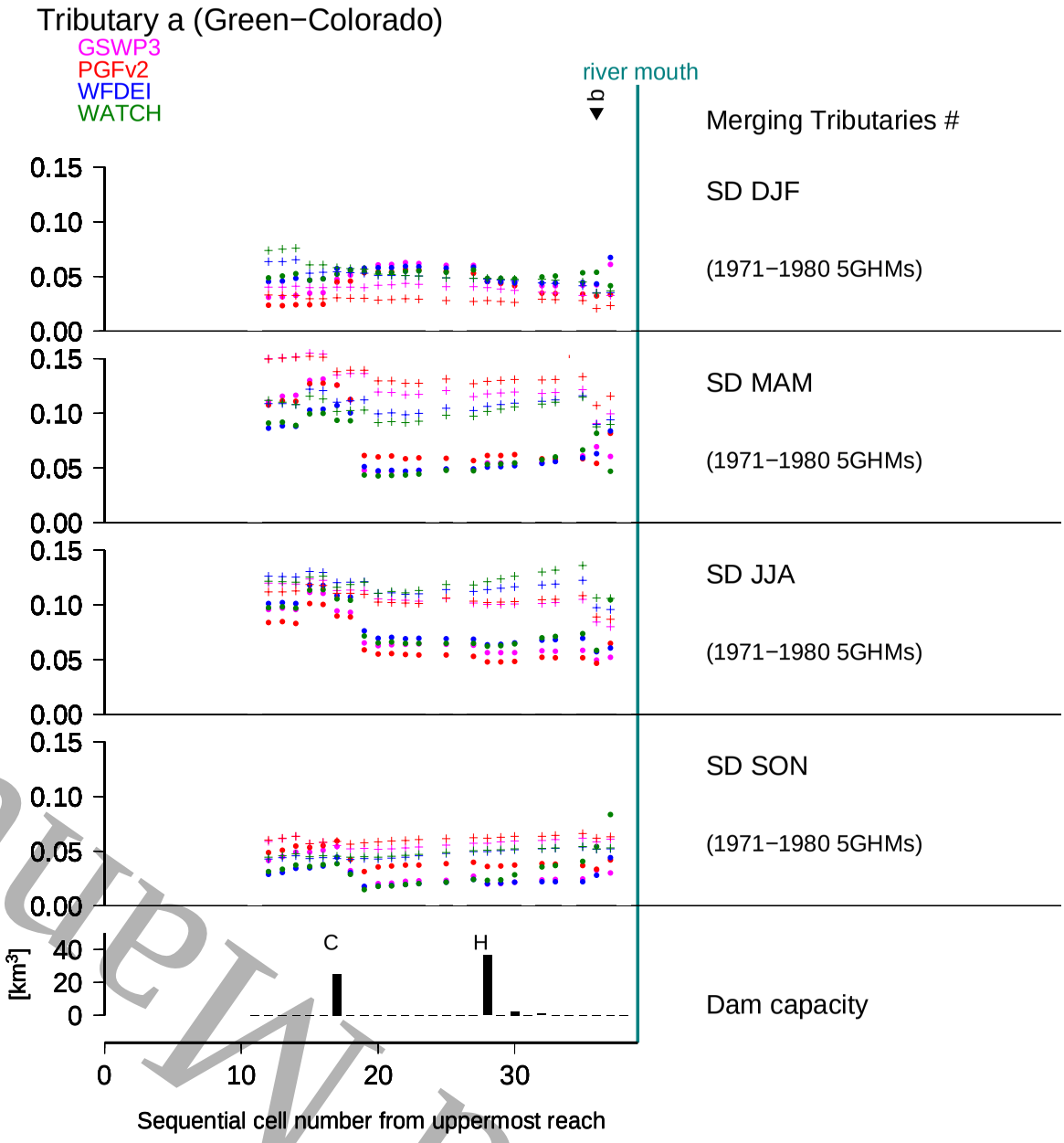

Figure 9. Same as Figure 8 but for the longitudinal section along the Green-Colorado River. The seasonal fraction for each GHM was shown in Figure 5. The horizontal axis is the sequential cell number (SCN) from the uppermost reach of the Green River (as indicated in Figure 1). Glen Canyon (C) and Hoover (H) Dams are located at SCNs 17 and 28, respectively.

4. Discussion

4.1. Interpretation of hydrological simulation of river discharge regulated by dams

In this study, we examined the uncertainties among GHMs and the potential errors along river channels and obtained new insights and caveats through case studies for the interpretation of simulated river discharge specific to regulated rivers.

First, differences in the seasonal fraction were detected among the GHMs. This is likely attributable to two factors: natural flow and dam regulation. (1) Regarding natural flow, differences among the GHMs were expected based on previous studies (e.g., Haddeland *et al* , 2011). Moreover, difficulties in reproducing snowmelt may also be a source of intermodel differences because both river basins used in this study are covered by a thick snowpack in winter (e.g., Slater *et al* , 2001; Rutter *et al* , 2009). In fact, over the catchment areas of Fort Peck Dam and Glen Canyon Dam, winter precipitation occurs as snow (Figures B1 and B2, respectively). Small differences in meteorological conditions (especially temperature) triggering snow melt can result in divergence in the timing of floods.

(2) Regarding dam regulation, dams fundamentally alter the timing of flow without changing absolute volumes of water when the dam capacity is large compared to the mean annual flow, and when secondary effects (local inflow to the dam, evaporation loss from the water surface, withdrawal or diversion for water supply and so forth) are regarded as sufficiently small compared with river flow. That is, the long-term average annual volume of discharge is considered to be independent of the dam operation scheme. To the best of our knowledge, generic dam operation schemes are fundamentally based on a function of inflow to the dam and the water demand for each purpose of the dam (Hanasaki *et al* , 2006; Haddeland *et al* , 2006). Recall that the natural inflow was different among the GHMs. Even if the same dam capacity was adopted for multiple GHMs, differences in dam inflows can cause simulated river discharge to diverge downstream among the GHMs due to different responses to the simulated inflow.

There are intrinsic difficulties in constructing advanced generic schemes for dam regulation. Dam operation data are generally not publicly available. The dams along the Missouri River represent a very rare case in which the operation strategy is publicly available (US Army Corps, 2006). Although the actual operation of multiple dams in the same river basin is more complex because they are mutually linked (e.g., Nagy *et al* , 2002), this is not taken into account by the operation schemes implemented in the GHMs.

In this study, we used the seasonal fractions of river flow, not the absolute seasonal volumes, because Haddeland *et al* (2011) revealed that annual river discharge values also differ among GHMs with a wide range of runoff coefficients (runoff divided by precipitation) at the basin scale. By introducing the seasonal fraction normalized by the annual volume, we expect that seasonal dam operation behavior can be focused on by artificially cancelling the effect of differences among runoff coefficients.

Secondly, the case studies also showed decreasing intermodel differences moving

toward the lower reaches. This probably reflects the fact that averaging over a larger catchment area helps stabilize simulated river discharges, which are susceptible to local instabilities. In most hydrological analyses, the performance of a simulation is evaluated at gauge stations at the farthest reach of the river, because river flow there reflects the overall characteristics of the catchment area, namely, the whole river basin. This is convenient for obtaining an overall picture of the basin. However, we should keep in mind that larger intermodel discrepancies may exist at gauge stations upstream.

In this paper, we only discussed two case-study river basins. However, notice that we used only simulated river discharge, one of fundamental variables in hydrological simulations, to depict dam functions. Visualizing methods like Figures 3 and 5 are applicable to other river basins in the world, if river discharge data are available.

GHMs will play an increasingly important role in evaluating hydrological impacts on societies as global climates and environments change rapidly, because they can simulate water availability with human interventions at the global scale under given meteorological conditions. Currently, most rivers flowing through populated areas are regulated by dams. In the future, GHMs will still strongly rely on generic dam operation schemes to make them applicable at the global scale.

Both river discharge and storage in dams have been attracting interest. For example, hydropower generation is increasingly seen as a means of reducing the emission of greenhouse gases while meeting the increasing demand for electricity. Hydrological simulation can also be used to assess the future potential of hydropower generation (e.g., Lehner *et al* , 2005; Masaki *et al* , 2014; Liu *et al* , 2016). Moreover, large dams create an anaerobic environment at the bottom and emit methane to the atmosphere, especially in tropical regions (Fearnside, 1995; Abril et al., 2005; Kemenes et al., 2007). From an ecological viewpoint, aquatic environments and ecosystems are of great concern. Physical aspects (e.g., surface area, level, and storage) of the water surface are observed with various techniques, such as remote sensing imagery, satellite altimetry, and bathymetry, to study aquatic environments. Accurate estimation of dam storage using GHMs will be welcomed not only by hydrological scientists, but also by those in the related fields of environmental and social sciences.

4.2. Future improvement of GHMs with regulated rivers

There is a considerable trade-off, specific to GHMs, in pursuing global applicability and high-performance reproductions of observed river discharge at the cost of ignoring local diversity in the natural and social environments of each river basin. In practice, GHMs with a spatial resolution of $0.5^\circ \times 0.5^\circ$ can neither consider all local conditions nor implement dam operation schemes for the over 60,000 dams across the world. This is in clear contrast to regional hydrological models (RHMs), which can be tuned to a certain river basin and its environment, and can potentially implement an actual dam manipulation scheme. We consider there to be no essential differences between GHMs and RHMs in terms of model structure, analytical scheme, and the physics

of hydrological processes, as summarized in Table A3 of Hattermann *et al* (2016). Moreover, as discussed in detail in Hattermann *et al* (2016), the high performance of RHMs is considered to be partly due to calibration, which poses the simultaneous risk of over-calibration. In addition, Gosling *et al* (2016) found little difference in the simulations from an ensemble of GHMs and an ensemble of RHMs, when the individual models were forced with meteorological projections from climate models.

Despite such a trade-off relationship, high-accuracy reproduction of the world's river discharge using GHMs should be the ultimate goal to improve our understanding of surface waters. Multimodel intercomparison studies carried out in the last several years have revealed broader differences among GHMs. It is critical to examine the reasons for this, identify sources of error, and improve models (e.g., Huber *et al* , 2014), as is being attempted currently. As we showed in this study, dam regulation is a source of differences among GHMs. Amending these models would result in high-performance simulations and greatly benefit hydrological science.

Some of our intercomparison results are degraded because of inconsistencies in simulation settings and conditions (i.e., the location of major dams), as we showed earlier. However, we emphasize that, in any types of gridded dam location data (Table A2), which stemmed from the GRanD data, dams were not simply placed on a land cell where the actual geographical coordinates indicated. The location was adjusted to harmonize the river channels, catchment area, and so on. The adjustment to different extents or with different priorities diverged the dam location. There are fundamental difficulties for such multimodel intercomparisons when using completely identical conditions, because each GHM has a different model structure and development history. On the other hand, this study provides a good opportunity to consider how dam locations should be assigned in the river network for hydrological simulations.

This paper is the first study that reports intermodel comparison of dam functions. Uncertainties always accompany with hydrological simulations. This study reveals that dam function, as well as natural flow, affects uncertainties in hydrological simulations. In particular, since this study used historical meteorological data, simulated results can be directly compared with observation. Such validation is crucial for future projections of climate change impacts because of substantial difficulties in validating future simulation results.

Despite such difficulties, this study revealed that seasonality in simulated river flow is the result of both simulated natural flow and flow regulation by dams. There are still arguments about the level of consistency needed in analysis settings for intercomparisons. If dam settings across GHMs are perfectly consistent, then more meaningful intercomparisons of dam functions can be realized, from shorter (e.g., heavy rainfall and flood prevention by dams) to longer (e.g., seasonal flow regulation at large dams) time scales.

5. Conclusions

We performed an intercomparison of river discharge regulated by large dams along the Missouri-Mississippi and Green-Colorado Rivers in the United States to examine the impacts of dam operation on river flow. Seasonality in river discharge was examined in longitudinal sections of the rivers to visualize seasonal modulation by dams and its downstream effects. We confirmed that the magnitude of dam regulation differs among GHMs. The differences in flow regulation are attributable not only to dam operation schemes but also to the magnitude of the simulated dam inflow and subsequent dam storage. Each GHM has advantages and disadvantages in reproducing the seasonality of river discharge. We observed decreasing intermodel discrepancies in the seasonal fraction towards the lower reaches of rivers in this study. Since model characteristics were more clearly detected in upper reaches, intermodel comparisons should be made in both upstream and downstream sections.

This is the first study to examine the performance of dam regulation in hydrological simulations using multiple models and forcings. Here, we demonstrated that model characteristics of the magnitude of flow regulation are formed not only by the dam operation itself, but also by the river discharge under natural (i.e., unregulated) conditions. GHMs incorporating dam operation are becoming increasingly important for hydrological simulations because most major global rivers are regulated by dams. This study implies that both natural river flow simulations and dam operation schemes must be improved to increase the performance of regulated river flow simulations.

GHMs have a trade-off between high performance and global applicability. Steady efforts toward improved modeling of both the natural flow and human impact will expand their applicability and improve the reliability of global hydrological simulations in an era characterized by increasing concern about the global environment.

Acknowledgments

We acknowledge two anonymous reviewers for their fruitful suggestions to this manuscript. This research was supported by the Environment Research and Technology Development Fund (S-10) of the Ministry of the Environment, Japan. This work has been conducted under the framework of ISIMIP. Observation data on river discharge were provided from the Global Runoff Data Center (GRDC) and from the United States Geological Survey (USGS) through the web interface, National Water Information System (http://nwis.waterdata.usgs.gov/nwis). Dam operation data were provided from the US Army Corps of Engineers, Northwest Division.

References

Abril G, Guérin F, Richard S, Delmas R, Galy-Lacaux C, Gosse P, Tremblay A, Varfalvy L, Dos Santos M A and Matvienko B 2005 Carbon dioxide and methane emissions and the carbon budget of a 10-year old tropical reservoir (Petit Saut, Grench Guiana) *Glob. Biogeochem. Cycles* **19** GB4007

Adeloye A J 2012 Hydrological sizing of water supply reservoirs *Encyclopedia of Lakes and Reservoirs* (ed L Bengtsson, R W Herschy and R W Fairbridge) 346–55 (Dordrecht, The Netherlands: Springer)

Avakyan A B and Iakovleva V B 1998 Status of global reservoirs: The position in the late twentieth century *Lakes Reserv. Res. Manag.* **3** 45–52

Biemans H, Haddeland I, Kabat P, Ludwig F, Hutjes R W A, Heinke J, von Bloh W and Gerten D 2011 Impacts of reservoirs on river discharge and irrigation water supply during the 20th century *Water Resour. Res.* **47** W03509

Bierkens M F P 2015 Global hydrology 2015: State, trends, and directions *Water Resour. Res.* **51** 4923–47

Compo G P *et al* 2011 The twentieth century reanalysis project *Q. J. R. Meteorol. Soc.* **137** 1–28

Dankers R *et al* 2014 First look at changes in flood hazard in the Inter-Sectoral Impact Model Intercomparison Project ensemble *Proc. Nat. Acad. Sci. U.S.A.* **111** 3257–61

Dee D P *et al* 2011 The ERA-Interim reanalysis: configuration and performance of the data assimilation system *Q. J. R. Meteorol. Soc.* **137** 553–597

Döll P and Lehner B 2002 Validation of a new global 30-min drainage direction map *J. Hydrol.* **258** 214–31

Fearnside P M 1995 Hydroelectric dams in the Brazilian Amazon as sources of 'greenhouse' gases *Environ. Conserv.* **22** 7–19

Goldewijk K K, Beusen A, van Drecht G and de Vos M 2011 The HYDE 3.1 spatially explicit database of human-induced global land-use change over the past 12,000 years *Global Ecol. Biogeogr.* **20** 73–86

Gosling S N *et al* 2016 A comparison of changes in river runoff from multiple global and catchment-scale hydrological models under global warming scenarios of 1°C, 2°C and 3°C *Climatic Change* doi:10.1007/s10584-016-1773-3

Haddeland I, Skaugen T and Lettenmaier D P 2006 Anthropogenic impacts on continental surface water fluxes *Geophys. Res. Lett.* **33** L08406

Haddeland I *et al* 2011 Multimodel estimate of the global terrestrial water balance: setup and first results *J. Hydrometeorol.* **12** 869–84

Hanasaki N, Kanae S and Oki T 2006 A reservoir operation scheme for global river routing models *J. Hydrol.* **327** 22–41

Hanasaki N, Kanae S, Oki T, Masuda K, Motoya K, Shirakawa N, Shen Y and Tanaka K 2008a An integrated model for the assessment of global water resources – Part 1: Model description and input meteorological forcing *Hydrol. Earth Syst. Sci.* **12** 1007–25

Hanasaki N, Kanae S, Oki T, Masuda K, Motoya K, Shirakawa N, Shen Y and Tanaka K 2008b An integrated model for the assessment of global water resources – Part 2: Applications and assessments *Hydrol. Earth Syst. Sci.* **12** 1027–37

Hattermann F F *et al* 2016 Cross-scale intercomparison of climate change impacts simulated by regional and global hydrological models in eleven large river basins *Climatic Change* (submitted)

Huber V *et al* 2014 Climate impact research: beyond patchwork *Earth Syst. Dynam.* **5** 399–408

The Inter-Sectoral Impact Model Integration and Intercomparison Project 2015 ISIMIP2a Simulation protocol (https://www.isimip.org/protocol/)

International Commission on Large Dams 2016 (http://www.icold-cigb.org/GB/World_register/general_synthesis.asp)

Kalnay E *et al* 1996 The NCEP/NCAR 40-year reanalysis project *Bull. Am. Meteorol. Soc.* **77** 437–71

Kemenes A, Forsberg B R and Melack J M 2007 Methane release below a tropical hydroelectric dam *Geophys. Res. Lett.* **34** L12809

Kim H 2014 (http://hydro.iis.u-tokyo.ac.jp/GSWP3/index.html)

Lehner B, Czisch G and Vassolo S 2005 The impact of global change on hydropower potential of Europe: a model-based analysis *Energy Policy* **33** 839–55

Lehner B *et al* 2011a High-resolution mapping of the world's reservoirs and dams for sustainable river-flow management *Front. Ecol. Environ.* **9** 494–502

Lehner B *et al* 2011b Global Reservoir and Dam (GRanD) database, Technical documentation Version 1.1 (http://www.gwsp.org/fileadmin/downloads/GRanD_Technical_Documentation_v1_1.pdf)

Liu X, Tang Q, Voisin N and Cui H 2016 Projected impacts of climate change on hydropower potential in China *Hydrol. Earth Syst. Sci.* **20** 3343–59

Masaki Y, Hanasaki N, Takahashi K and Hijioka Y 2014 Future changes in theoretical hydropower potential and hydropower generation based on river flow under climate change *J. Japan Soc. Civil Engineers, Ser. G* **70** I_111–I_120 doi:10.2208/jscejer.70.I_111 (in Japanese)

Masaki Y *et al* 2016 (Paper I) Intercomparison of regulated river discharge among multiple hydrological models under multiple forcings along two major rivers in the United States — (I) Effects of multiple forcings *Environ. Res. Lett.* (submitted)

Müller Schmied H, Eisner S, Franz D, Wattenbach M, Portmann F T, Flörke M and Döll P 2014 Sensitivity of simulated global-scale freshwater fluxes and storages to input data, hydrological model structure, human water use and calibration, *Hydrol. Earth Syst. Sci.* **18** 3511–38

Müller Schmied H *et al* 2016a Variations of global and continental water balance components as impacted by climate forcing uncertainty and human water use *Hydrol. Earth Syst. Sci.* **20** 2877–98

Müller Schmied H, Zhao F, and Ostberg S 2016b Visualization of the three reservoir datasets used in ISIMIP2a, http://arcg.is/2cn93Km

Nagy I V, Asante-Duah K and Zsuffa I 2002 *Hydrological dimensioning and operation of reservoirs: Practical design concepts and principles* p 225 (Dordrecht, The Netherlands: Kluwer Academic Publishers)

Nazemi A and Wheater H S 2015a On inclusion of water resource management in Earth system models – Part 1: Problem definition and representation of water demand *Hydrol. Earth Syst. Sci.* **19** 33–61

Nazemi A and Wheater H S 2015b On inclusion of water resource management in Earth system models – Part 2: Representation of water supply and allocation and opportunities for improved modeling *Hydrol. Earth Syst. Sci.* **19** 63–90

Nijssen B, O'Donnell G M, Lettenmaier D P, Lohmann D and Wood E F 2001 Predicting the discharge of global rivers *J. Clim.* **14** 3307–23

Nilsson C, Reidy C A, Dynesius M and Revenga C 2005 Fragmentation and flow regulation of the world's large river systems *Science*, **308**, 405–08

Norton P A, Anderson M T and Stamm J F 2014 *Trends in annual, seasonal, and monthly streamflow characteristics at 227 streamgages in the Missouri River Watershed, water years 1960–2011* (US Geological Survey Scientific Investigations Report 2014-5053) p 128 (Reston, VA, USA: US Geological Survey)

Portmann, F. T., S. Siebert and P. Döll (2010), MIRCA2000–Global monthly irrigated and rainfed crop areas around the year 2000: A new high-resolution data set for agricultural and hydrological modeling, Glob. Biogeochem. Cycles, 24, GB1011.

Prudhomme C *et al* 2014 Hydrological droughts in the 21st century, hotspots and uncertainties from a global multimodel ensemble experiment *Proc. Nat. Acad. Sci. U.S.A.* **111** 3262–67

Rhodes S L, Ely D and Dracup J A 1984 Climate and the Colorado River: The limits of management *Bull. Amer. Meteorol. Soc.* **65** 682–91

Rippl W 1883 The capacity of storage-reservoirs for water-supply *Minutes of Proceedings* **71** 270–78

Rost S, Gerten D, Bondeau A, Lucht W, Rohwer J and Schaphoff S 2008 Agricultural green and blue water consumption and its influence on the global water system *Water Resour. Res.* **44** W09405

Rutter N *et al* 2009 Evaluation of forest snow processes models (SnowMIP2) *J. Geophys. Res.* **114** D06111

Schewe J *et al* 2014 Multimodel assessment of water scarcity under climate change *Proc. Nat. Acad. Sci. U.S.A.* **111** 3245–50

Sheffield J, Goteti G and Wood E F 2006 Development of a 50-year high-resolution global dataset of meteorological forcings for land surface modeling *J. Climate* **19** 3088–11

Slater A G *et al* 2001 The Representation of Snow in Land Surface Schemes: Results from PILPS 2(d) *J. Hydrometeorol.* **2** 7–25

Sperna Weiland F C, van Beek L P H, Kwadijk J C J and Bierkens MFP 2010 The ability of a GCM-forced hydrological model to reproduce global discharge variability *Hydrol. Earth Syst. Sci.* **14** 1595–621

Stone M C, Hotchkiss R H, Hubbard C M, Fontaine T A, Mearns L O and Arnold J G 2001 Impacts of climate change on Missouri River Basin water yield *J. Amer. Water Resour. Assoc.* **37**, 1119–29

Tang Q, Oki T, Kanae S and Hu H 2007 The influence of precipitation variability and partial irrigation within grid cells on a hydrological simulation *J. Hydrometeorol.* **8** 499–512

United States Army Corps of Engineers 2006 *Missouri River Mainstem Reservoirs System master water control manual (Revision 1)* p 432 (Omaha, NE, USA: Northern Division of the United States Army Corps of Engineers)

United States Government Accountability Office 2014 *Missouri river flood and drought* (Report to Congressional Requesters GAO-14-741) p 50 (Washington D.C., DC, U.S.A.: US Government Accountability Office)

Uppala S M *et al* 2005 The ERA-40 re-analysis *Q. J. R. Meteorol. Soc.* **131** 2961–3012

Vörösmarty C J, Sharma K P, Fekete B M, Copeland A H, Holden J, Marble J and Lough J A 1997 The storage and aging of continental runoff in large reservoir systems of the world *Ambio* **26** 210–19

Wada Y *et al* 2013 Multimodel projections and uncertainties of irrigation water demand under climate change *Geophys. Res. Lett.* **40** 4626–32

Wada Y, Wisser D and Bierkens M F P 2014 Global modeling of withdrawal, allocation and consumptive use of surface water and groundwater resources *Earth Syst. Dynam.* **5** 15–40

Weedon G P, Gomes S, Viterbo P, Österle H, Adam J C, Bellouin N, Boucher O and Best M 2010 *The WATCH Forcing Data 1958-2001: a meteorological forcing dataset for land surface- and hydrological models* (WATCH Technical Report 22) p 41 (www.eu-watch.org/publications)

Weedon G P, Balsamo G, Bellouin N, Gomes S, Best M J and Viterbo P 2014 The WFDEI meteorological forcing data set: WATCH Forcing Data methodology applied to ERA-Interim reanalysis data *Water Resour. Res.* **50** 7505–14

Yasutomi N, Hamada A and Yatagai A 2011 Development of a long-term daily gridded temperature dataset and its application to rain/snow discrimination of daily precipitation *Global Environmental Research*, **15**, 165–72